Journal of Biological Methods | **2020** | **Vol**. 7(4) | e139
DOI: 10.14440/jbm.2020.336

ARTICLE

An adapted novel flow cytometry methodology to delineate types of cell death in airway epithelial cells

Samuel T. Montgomery[1], Stephen M. Stick[1,2,3,5], Anthony Kicic[1,2,3,4,5]

[1]Faculty of Medicine and Health Science, University of Western Australia, Western Australia 6009, Australia
[2]Telethon Kids Institute, University of Western Australia, Western Australia 6009, Australia
[3]Department of Respiratory and Sleep Medicine, Perth Children's Hospital, Western Australia 6009, Australia
[4]School of Public Health, Curtin University, Western Australia 6102, Australia
[5]Centre for Cell Therapy and Regenerative Medicine, School of Medicine and Pharmacology, University of Western Australia, Western Australia 6009, Australia

Corresponding author: Anthony Kicic, Email: anthony.kicic@telethonkids.org.au

Competing interests: The authors have declared that no competing interests exist.

Abbreviations used: A5, annexin V; AEC, airway epithelial cells; CF, cystic fibrosis; CFTR, cystic fibrosis transmembrane conductance regulator; FSC, forward scatter; h, hours; IL, interleukin; min, minutes; MOI, multiplicity of infection; PANX1, pannexin 1; PI, propidium iodide; qPCR, quantitative polymerase chain reaction; RIP1K, receptor-interacting serine/threonine-protein kinase 1; RV, human rhinovirus; SSC, side scatter; TP3, TO-PRO-3; UV, ultraviolet

Received April 30, 2020; Revision received September 30, 2020; Accepted October 30, 2020; Published November 11, 2020

ABSTRACT

Current methodologies to measure apoptotic and necrotic cell death using flow cytometry do not adequately differentiate between the two. Here, we describe a flow cytometry methodology adapted to airway epithelial cells (AEC) to sufficiently differentiate apoptotic and necrotic AEC. Specifically, cell lines and primary AEC (n = 12) were permeabilized or infected with rhinovirus 1b (RV1b) over 48 h. Cell death was then measured *via* annexin V/propidium iodide (A5/PI) or annexin V/TO-PRO-3 (A5/TP3) staining using a novel flow cytometry and gating methodology adapted to AEC. We show that A5/PI staining could not sufficiently differentiate between types of cell death following RV1b infection of primary AEC. However, A5/TP3 staining was able to distinguish six cell death populations (viable, necrotic, debris, $A5^+$ apoptotic, $A5^-$ apoptotic, apoptotic bodies) after permeabilization or infection with RV1b, with phenotypic differences were observed in apoptotic populations. Collectively, using a staining and gating strategy never adapted to AEC, A5/TP3 could accurately differentiate and quantify viable, necrotic, and apoptotic AEC following RV1b infection.

Keywords: airway epithelium, cell death, rhinovirus, flow cytometry

INTRODUCTION

Cystic fibrosis (CF) lung disease is characterized by neutrophilic airway inflammation associated with progressive airway remodeling which begins early in life, even in absence of bacterial infection [1]. In infants with CF, human rhinovirus (RV) is the most commonly detected virus [2] and while children with and without CF have similar rates of viral infection, the effects and clinical outcomes of these infections are more severe in those with CF [3]. The primary target of RV infection remains the airway epithelial cells (AEC), and although it is capable of infecting other cells types including monocytes and macrophages, preferentially replicates in the airway epithelium [4]. Replication of RV has been shown to be significantly increased in CF AEC when compared to non-CF AEC [5]. Of significance, is the observation that AEC from children with CF elicit a damped apoptotic response following infection compared to non-CF controls, even when normalized to viral load and overall epithelial cell death [5]. It has also been recently observed that the rhinovirus 3C protease disrupts the apoptotic response to RV infection through cleavage of receptor-interacting serine/threonine-protein kinase 1 (RIPK1), resulting in a necrosis-like phenotype of cell death [6].

Studies utilizing βENaC-overexpressing mice with CF-like lung disease have suggested a link between mucus obstruction, necrosis of AEC, and sterile neutrophilic inflammation driven by the release of interleukin-1 alpha (IL-1α) from necrotic cells activating the interleukin-1 receptor (IL-1R) signaling pathway [7]. These findings suggest that triggering IL-1R signaling *via* IL-1α may be an important mechanism in early CF inflammation. Previous work from AREST CF has established that IL-1α is associated with structural lung disease specifically in the absence of bacterial infection [8], suggesting a role for IL-1α released from necrotic cells in the inflammatory cascade observed in the early

How to cite this article: Montgomery ST, Stick SM, Kicic A. An adapted novel flow cytometry methodology to delineate types of cell death in airway epithelial cells. *J Biol Methods* 2020;7(4):e139. DOI: 10.14440/jbm.2020.336

CF airway. Knowing that RV infections result in AEC cell death drive inflammation in early life CF, it is imperative to be able to accurately determine viable, necrotic, and apoptotic cells in this population. However, existing assays lack accuracy in determining these parameters.

Currently, propidium iodide (PI) is typically used with annexin V (A5) for assessing cell death in flow cytometry, to discriminate between live, apoptotic and necrotic cell populations [9]. A5 binds to phosphatidylserine, which is translocated to the outer layer of the plasma membrane during early apoptosis, while PI fluoresces when bound to DNA. Cells with intact membranes exclude PI, allowing discrimination of viable and early apoptotic cells [9]. Late apoptotic and necrotic cells have increased cell permeability and disrupted membranes, which allows PI into the cell to discriminate dead cells from live [10]. However, apoptotic cells that are unable to be phagocytosed, such as *in vitro* cultures, undergo secondary apoptosis characterized by the same features as necrosis [11]. As a result, there is debate whether the $A5^+/PI^+$ quadrant relates to necrotic cells, late apoptotic cells, or secondary apoptotic cells, with the suggestion that conventional methodologies result in a false-positive rate of up to 40% [12]. Differentiation requires drug treatment blocking RIPK1 activation [13] or a RNase treatment which requires fixation prior to treatment [12], limiting experiments requiring live cells. As a result, the adaptation of a novel flow cytometry methodology to AEC was investigated using an alternative dye to PI, TO-PRO-3, to identify viable cells, three stages of cell death, and two subcellular fragments [14].

TO-PRO-3 uses pannexin 1 (PANX1) membrane channels activated during early stages of apoptosis for cell entry into early apoptotic cells [15], while entering membrane-permeabilized cells independent of PANX1 resulting in dramatically increased staining of membrane compromised cells [14]. This allows the identification of apoptotic cells independent of annexin V staining, as apoptotic cells can be discriminated from both viable and membrane-compromised cells *via* TO-PRO-3 staining. With the addition of annexin V, this methodology can identify both annexin-positive apoptotic cells and early apoptotic cells with PANX1 activation, but no phosphatidylserine externalization or annexin binding [14]. This methodology can also capture extracellular vesicles formed when apoptotic cells disassemble for phagocytosis called apoptotic bodies [14]. Apoptotic body formation potentially plays an important role in phagocytosis [16], and apoptotic bodies can transfer RNA, protein, and lipids between cells to facilitate cell-to-cell communication [17,18]. To determine the role of apoptotic bodies in disease settings, it is important be able to accurately identify these vesicles. In this study, this methodology was adapted for the first time to AEC to test the hypothesis that it would delineate types of cell death with greater certainty than the traditional A5/PI flow cytometry methodology.

MATERIAL AND METHODS

Study population

This study was approved by the relevant institutional Human Ethics Committees with written informed consent obtained from parents or guardians. Children with CF were recruited during annual early surveillance visits where cystic fibrosis transmembrane conductance regulator (CFTR) genotype were determined as part of newborn screening. Primary AEC samples from six clinically stable infants and children with CF (mean age 2.9 ± 1.8 years old; **Table S1**) were used where children with CF carried at least one Phe508 del allele, and 83% were homozygous. Furthermore, six healthy children without CF (mean age 3.8 ± 1.9 years old; **Table S1**) were recruited when attending hospital for elective non-respiratory related surgery.

Cell culture

Primary AEC samples were attained by brushing of the tracheal mucosa of children with a single-sheathed nylon bronchial cytology brush (BC 25105, Olympus, Australia) as previously described [5]. After collection, primary AEC cultures were established as conditionally reprogrammed cultures as previously described [19]. Also included in the study was a healthy non-CF AEC line $16HBE14o^-$ and equivalent CF AEC line CFBE41o—which were cultured as previously described [5].

Rhinovirus infection

Human rhinovirus 1b (RV1b) was propagated as previously described [20]. To simulate an acute RV infection *in vitro*, primary AEC were exposed to ~2.95×10^5 $TCID_{50}$/ml which equated to a multiplicity of infection (MOI) 3. To ensure responses were due to actively replicating virus, control AEC were exposed to UV-inactivated RV1b at MOI 3. After 48 h incubation, cells from all treatment conditions were collected for analysis *via* flow cytometry. Viral load of RV1b to confirm infection was measured after 24 h incubation *via* quantitative polymerase chain reaction (qPCR) as previously described [21] (**Fig. S1**).

Flow cytometry

A flow cytometry methodology to measure cell death and disassembly [14] was adapted for use with AEC. Briefly, AEC were detached from culture surfaces *via* gentle trypsinization using 0.25% (v/v final) trypsin (Lonza, Basel, Switzerland). Cell supernatant was centrifuged at 1000 *g* for 3 min at 4°C and pelleted cells combined with trypsinized cells. Combined cells were then pelleted by centrifugation at 500 *g* for 7 min at 4°C and resuspended at a concentration of 10^6 cells/ml in annexin binding buffer (Thermo Fisher Scientific, Waltham, MA, USA). Cells used as positive controls for dead cells were fixed and permeabilized by incubation with 3.7% paraformaldehyde for 10 min. Tubes containing 100 µl of cell suspension were stained for 15 min with 100 µl of annexin V/AlexaFluor488 (Thermo Fisher Scientific, Waltham, MA, USA) (1:40 v/v) and propidium iodide (1 µg/ml final concentration) (Thermo Fisher Scientific, Waltham, MA, USA) in annexin binding buffer or 100 µl of annexin V/AlexaFluor488 (1:40 v/v) and TO-PRO-3 (10 µM final concentration) (Thermo Fisher Scientific, Waltham, MA, USA) in annexin binding buffer. Flow cytometry was performed on a FACSCanto II flow cytometer (BD Biosciences, Franklin Lakes, NJ, USA). Acquisition gate was set to record 2×10^4 events total for each sample. Analysis was performed using FlowJo software v10.4 (FlowJo LLC, Ashland, OR, USA).

Gating strategies

A5/PI data was analyzed by excluding doublets, and sorting events into $A5^-/PI^-$, $A5^+/PI^-$, $A5^-/PI^+$, and $A5^+/PI^+$ quadrants. A5/TP3 data was analyzed using a novel flow cytometry analysis adapted in this study for epithelial cells that uses a seven step gating strategy to separate events into six populations: viable, necrotic, $A5^+$ apoptotic, $A5^-$ apoptotic, apoptotic bodies and cellular debris (**Fig. 1**) [14]. Positive staining was determined *via* single staining of fixed AEC using both A5 and TP3 and

gating determined accordingly. Cut-offs used for forward scatter (FSC) and side scatter (SSC) during analysis to delineate an intact cell were 5 × 10^4, with everything above termed positive (+) and everything below negative (−). Expected levels of A5 and TP3 staining for each population are outlined in **Table 1**. A5/TP3 data were analyzed *via* the following pipeline: first, data was separated into $TP3^+$ events and other events (**Fig. 1A**). The $TP3^+$ events were sorted by FSC into necrotic events (FSC^+) (**Fig. 1B**). The other events were then separated by SSC and A5 into $A5^-/SSC^+$ and other events (**Fig. 1C**) The $A5^-/SSC^+$ events were then sorted into viable ($FSC^+/TP3^-$) and $A5^-$ apoptotic events ($TP3^+$) (**Fig. 1D**). The other events were then separated into $A5^+$ and $A5^-$ (**Fig. 1E**), with the $A5^-$ then sorted by FSC into cellular debris (FSC^-) (**Fig. 1F**). The $A5^+$ was then sorted by FSC into $A5^+$ apoptotic events (FSC^+) and apoptotic bodies (FSC^-) (**Fig. 1G**).

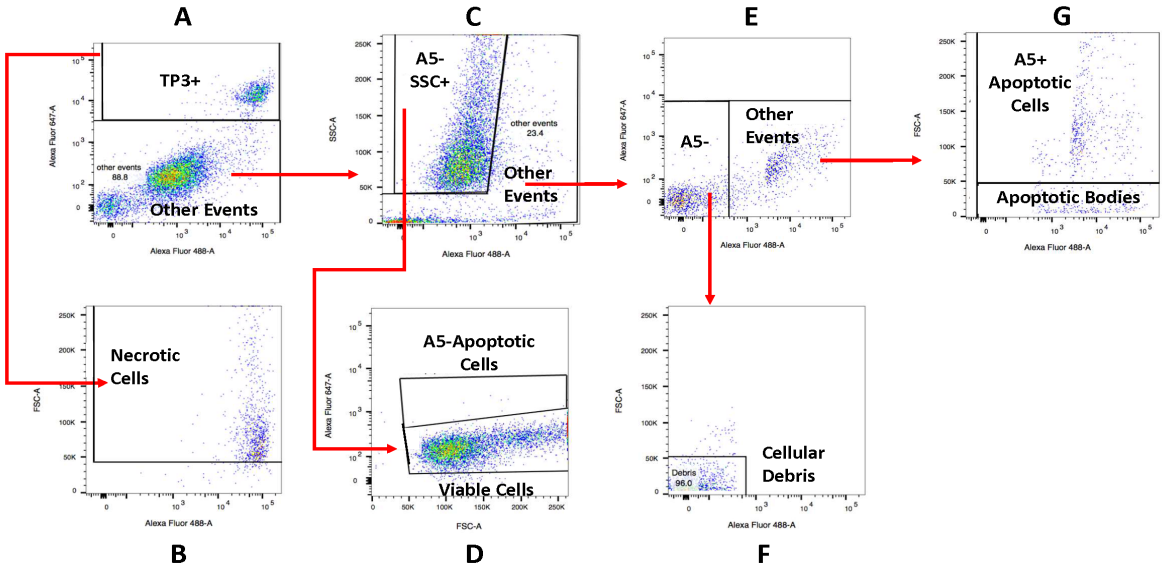

Figure 1. A5/TP3 gating and data analysis for differentiation of a sample into six populations. A. Data was sorted into $TP3^+$ events and other events. **B.** The $A5^+/TP3^+$ events were sorted by FSC into necrotic events (FSC^+). **C.** The $A5^-/TP3^-$ events were then separated by SSC and A5 into $A5^-/SSC^+$ and other events. **D.** The $A5^-/SSC^+$ events were then sorted into viable ($FSC^+/TP3^-$) and $A5^-$ apoptotic events ($TP3^+$). **E.** The "other events" were then separated into $A5^+$ and $A5^-$, with the $A5^-$ then sorted by FSC into cellular debris (FSC^-) (F). **G.** The $A5^+$ events were then sorted by FSC into $A5^+$ apoptotic events (FSC^+) and apoptotic bodies (FSC^-).

Statistics

Statistical analyses were conducted using GraphPad Prism v7.04 (GraphPad Software, La Jolla, CA, USA). Comparisons between paired data were performed using paired *t*-tests presented as mean ± standard deviation, and Wilcoxon matched pairs signed rank tests presented as median (interquartile range) where appropriate. Comparisons between unpaired data were performed using unpaired *t*-tests with Welch's correction presented as mean ± standard deviation, and Mann-Whitney tests presented as median (interquartile range) where appropriate. A two tailed *P* value < 0.05 was considered statistically significant.

RESULTS

A5/PI staining cannot sufficiently differentiate between cell populations using flow cytometry

To differentiate between types of cell death using A5/PI staining, primary AEC were infected with RV1b for 48 h and measured *via* flow cytometry. RV infection moderately but not significantly reduced viable events ($A5^-/PI^-$) (**Fig. 2A**), had no effect on necrotic events ($A5^-/PI^+$) (**Fig. 2B**) nor any effect on apoptotic events ($A5^+/PI^-$) (**Fig. 2C**). Furthermore, although secondary necrotic events were elevated ($A5^+/PI^-$), this was not considered significant (**Fig. 2D**). At baseline, 21.6% ± 9.7% of total events were identified as undergoing secondary necrosis which only slightly increased following fixation (39.2% ± 15.7%). However, the minimal apoptotic events observed at baseline (0.74% ± 0.43%) was observed not to change following fixation (1.77% ± 1.53%). Additionally, A5/PI staining is unable to detect the presence of apoptotic bodies formed during cell death.

A5/TP3 staining allows differentiation between six cell populations following fixation

Since using the traditional $A5^+/PI^-$ staining resulted in a large proportion of double positive staining that was further compounded by highly variable staining between samples, another flow cytometry methodology was then trialed using AEC lines. Utilizing a submerged monolayer model that ensures a single population of basal airway epithelial cells we exposed them to a typical fixative to determine cell death responses. Results generated showed that staining with A5/TP3 allowed differentiation into six different populations, namely: viable events, necrotic events, debris, $A5^+$ apoptotic events, $A5^-$ apoptotic events, and apoptotic bodies. When quantified, fixed AEC had reduced viable events (67.69% ± 13.4% *vs.* 4.81% ± 10.1%; $P < 0.05$), increased necrotic events (12.69% ± 7.15% *vs.* 28.73% ± 16.9%; $P < 0.05$), de-

creased debris (4.11% ± 4.09% *vs*. 1.40 ± 1.24%; $P < 0.05$), increased A5$^+$ apoptotic events (9.81% ± 5.41% *vs*. 56.35% ± 26.7%; $P < 0.05$) and had no effect on A5$^-$ apoptotic events or apoptotic bodies (**Fig. 2E**). To determine the overall responses to fixation, cell line responses were grouped into "viable", "necrotic" and "apoptotic" events for analysis. Fixation of cell lines significantly reduced viable events (67.69% ± 13.43% *vs*. 4.81% ± 10.13%; $P < 0.05$) (**Fig. 2F**), significantly increased necrotic events (12.69% ± 7.15% *vs*. 28.73% ± 16.94%; $P < 0.05$) (**Fig. 2G**), and significantly increased apoptotic events (15.03 ± 8.01% *vs*. 64.53% ± 21.60%; $P < 0.05$) (**Fig. 2H**).

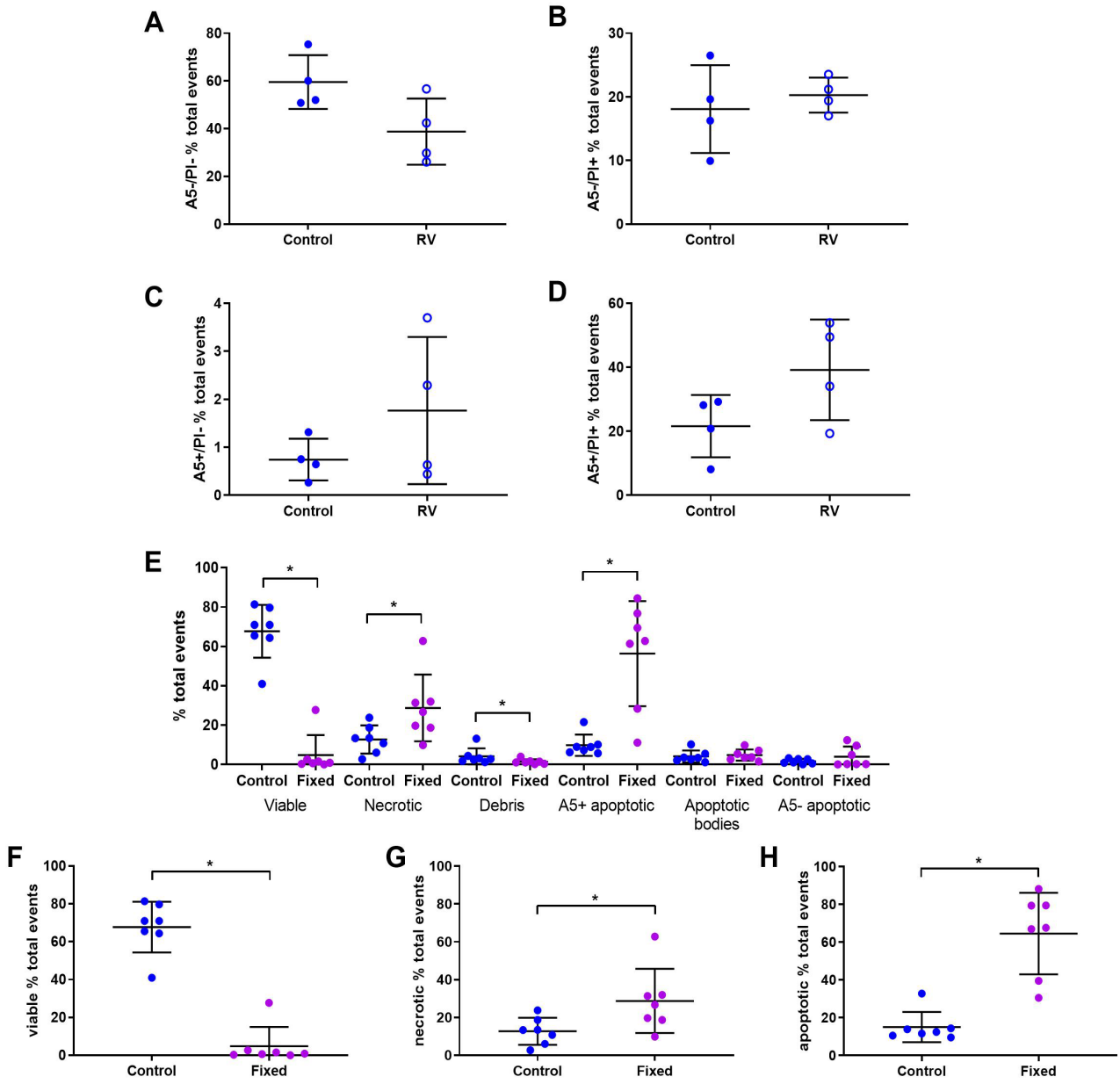

Figure 2. A5/PI cannot differentiate types of cell death in primary AEC but A5/TP3 is effective to differentiate viable, apoptotic, and necrotic AEC lines. Primary AEC ($n = 4$) were infected with RV1b for 48 h, collected and stained with A5/PI. RV1b infection decreased viable events (A), had no effect on necrotic events (B), had no effect on apoptotic events (C), and increased secondary necrotic events (D). AEC lines ($n = 7$) were collected, fixed with paraformaldehyde, and analyzed *via* flow cytometry. After fixation with paraformaldehyde, viable events were reduced compared to control, necrotic events were increased compared to control, debris was reduced compared to control, A5$^+$ apoptotic events were increased compared to control, and no changes in apoptotic bodies or A5$^-$ apoptotic events were observed compared to controls (E). When grouped into "viable", "necrotic", and "apoptotic" events, viable events were reduced compared to control (F), necrotic events were increased compared to control (G), and apoptotic events were increased compared to control (H). *$P < 0.05$.

A5/TP3 staining allowed measurement of viable, necrotic, and apoptotic events in primary AEC after fixation and RV infection

As differences were observed between control and fixed cell lines, primary AEC were then fixed, stained, and measured using flow cytometry to confirm initial results utilizing immortalized cell lines were translatable to primary cells. Fixation of primary AEC and staining with A5/TP3 resulted in similar staining to cell lines, with reduced viable events (79.53% ± 4.17% *vs*. 8.23% ±1.87%) (**Fig. 3A**), increased necrotic events (6.66% ± 3.52% *vs*. 56.02% ±13.0%) (**Fig. 3B**), and increased apoptotic events (9.90% ± 4.14% *vs*. 31.31% ± 11.24%) (**Fig. 3C**). To confirm A5/TP3 staining *via* flow cytometry could sufficiently detect differences after an infectious stimulus with clinical relevance, primary AEC were exposed to RV1b over 48 h. Viable events were significantly reduced compared to control following infection with RV1b for 24 h (61.35% ± 14.1% *vs*. 42.59% ± 16.5%; $P < 0.001$) and 48 h (58.07% ± 12.9% *vs*. 22.18 ± 13.6%; $P < 0.001$) (**Fig. 3D**). Additionally, viable events were significantly lower at control at 48 h compared to 24 h ($P < 0.05$), and lower following RV1b infection for 48 h compared to 24 h ($P < 0.05$). There were also increased necrotic events compared to control following infection with RV1b for both 24 h (8.560% ± 1.97% *vs*. 12.20 ± 4.09%, $P < 0.01$) and 48 h (10.12 ± 2.42% *vs*. 18.84% ± 6.42%, $P < 0.001$) (**Fig. 3E**). Additionally, necrotic events were significantly higher after 48 h of RV1b infection when compared to 24 h ($P < 0.001$). RV1b infection for 24 h also significantly increased debris (2.359% (1.62–2.53) *vs*. 6.725% (4.55–8.26); $P < 0.001$) (**Fig. 3F**) but had no effect on levels of $A5^+$ apoptotic events ($P > 0.05$) (**Fig. 3G**). However, RV1b infection significantly reduced $A5^-$ apoptotic events when compared to control after 24 h (3.58% ± 1.20% *vs*. 2.68% ± 1.08%; $P < 0.001$) and 48 h (4.33% ± 1.80% *vs*. 2.93% ±1.45%; $P < 0.05$) (**Fig. 3H**). Finally, apoptotic bodies were significantly increased when compared to control following RV1b infection for 24 h (9.92% (4.92–24.49) *vs*. 17.30% (9.84–28.49); $P < 0.05$) and 48 h (15.94% (7.05–29.81) *vs*. 39.28% (27.29–60.08); $P < 0.01$) (**Fig. 3I**). Thus, we report the ability to measure and differentiate events into viable, necrotic, and apoptotic populations and determine changes in cell viability and death in primary AEC following injurious stimuli like RV infection.

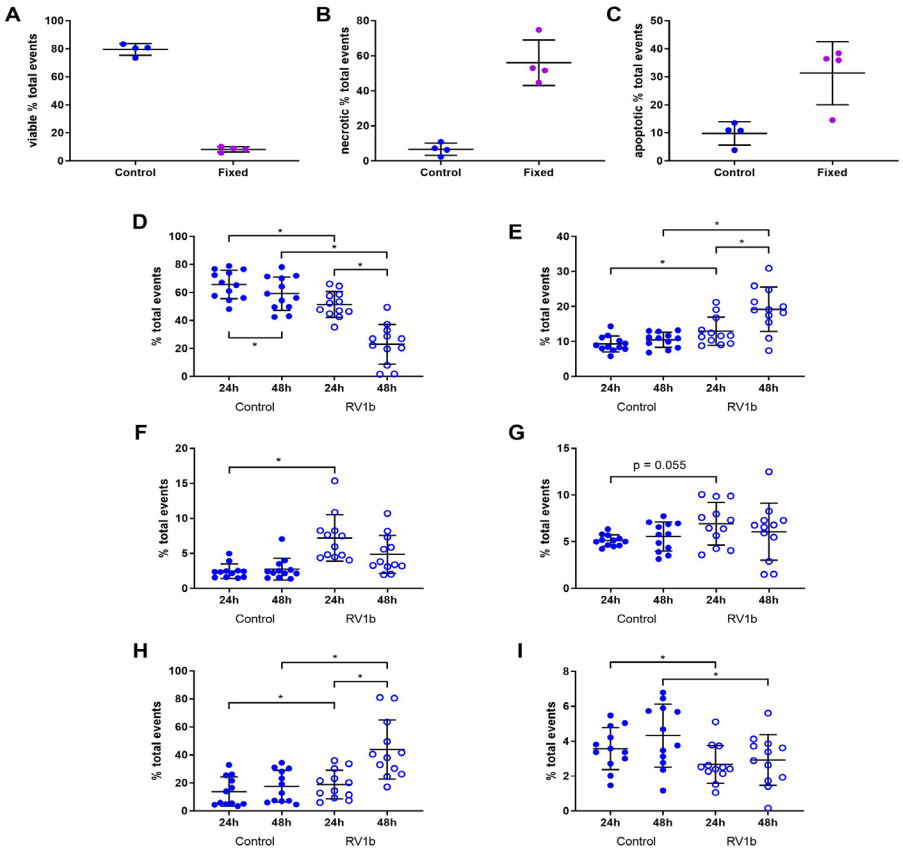

Figure 3. A5/TP3 staining in primary AEC results in measurable changes in viable, necrotic, and apoptotic events *via* flow cytometry. Primary AEC were collected, fixed with paraformaldehyde ($n = 4$) or infected with RV1b ($n = 12$) over 48 h, stained with A5/TP3, and analyzed *via* flow cytometry. After fixation with paraformaldehyde, viable events were reduced (A), necrotic events were increased (B), and apoptotic events were increased (C). RV1b infection: decreased viable after infection for 24 h and 48 h, with lower viable events at 48 h compared to 24 h in both control and RV1b (D), increased necrotic events after RV1b infection for 24 h and 48 h, with increased necrotic events at 48 h compared to 24 h (E), significantly increased debris following RV1b infection for 24 h (F) no change in $A5^+$ apoptotic events after RV1b infection over 48 h (G), significantly increased apoptotic bodies following RV1b infection for 24 and 48 h, with higher apoptotic bodies after 48 h of infection compared to 24 h (H), and significantly decreased $A5^-$ apoptotic events following RV1b infection for 24 h and 48 h (I). *$P < 0.05$.

A5/TP3 staining allows the observation in phenotypical differences in apoptotic cell disassembly

Following the optimization of the seven-step gating protocol for AEC, and the observation that RV infection of AEC resulted in increased apoptotic cell disassembly, we then determined phenotypical differences between non-CF and CF AEC infected with RV1b over 48 h. Infection with RV1b had no statistically significant effect on $A5^+$ apoptotic events after 24 h (**Fig. 4A**) or 48 h (**Fig. 4B**). However, RV1b infection significantly decreased $A5^-$ apoptotic events when compared to control after 24 h in non-CF (4.18% ± 1.10% *vs*. 3.31% ± 1.11%; $P < 0.01$) and CF AEC (2.98% ± 1.06% *vs*. 2.05% ± 0.62%; $P < 0.05$), with $A5^-$ apoptotic events following RV infection significantly lower in CF when compared to non-CF AEC ($P < 0.05$) (**Fig. 4C**). After 48 h of infection, there was a significant decrease in $A5^-$ apoptotic events in CF AEC (3.45% ± 1.67% *vs*. 2.11% ± 1.22%; $P < 0.01$) but not non-CF AEC (**Fig. 4D**). Additionally, after 48 h of infection $A5^-$ apoptotic events were significantly lower in CF AEC when compared to non-CF AEC (2.11% ±1.22% *vs*. 3.74% ± 1.25%; $P < 0.05$) (**Fig. 4D**). Finally, infection with RV1b for 24 h significantly increased apoptotic bodies in non-CF (15.23% (5.01–22.77) *vs*. 20.86% (13.99–31.15); $P < 0.05$) but not CF AEC (**Fig. 4E**). After 48 h, significantly increased apoptotic bodies were observed in both non-CF (21.20% (11.29–28.67) *vs*. 45.63% (36.77–67.80); $P < 0.05$) and CF AEC (7.35% (5.69–31.92) *vs*. 28.31% (22.71–50.66); $P < 0.05$) (**Fig. 4F**).

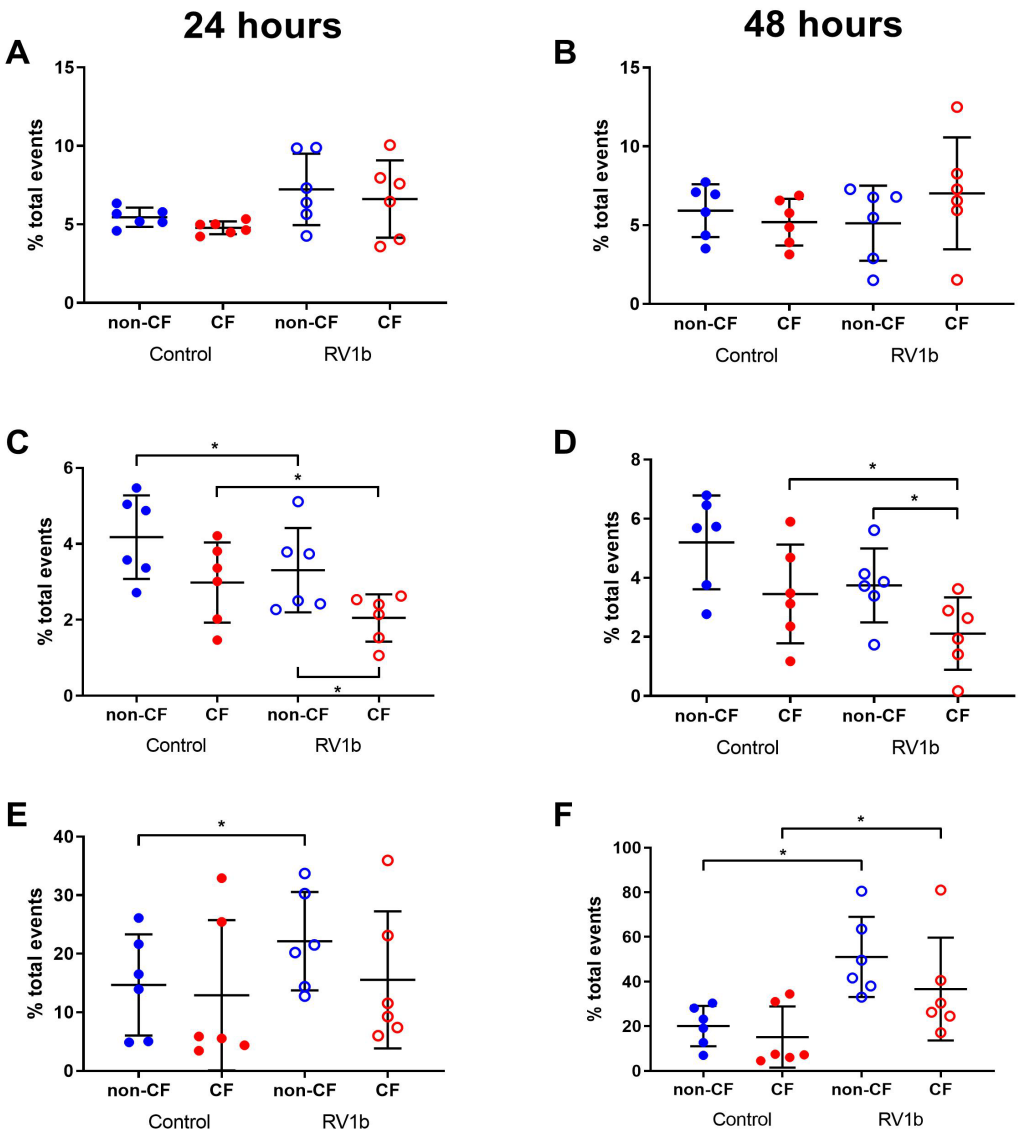

Figure 4. A5/TP3 staining in primary AEC results in measurable phenotypic differences in apoptotic populations. Non-CF ($n = 6$) and CF ($n = 6$) primary AEC were infected with RV1b over 48 h, stained with A5/TP3, and analysed *via* flow cytometry. RV1b infection: had no significant effect on $A5^+$ apoptotic events after 24 h (A) and 48 h (B), significant decreased $A5^-$ apoptotic events after 24 h in both non-CF and CF AEC, with significantly lower events in CF (C), significantly decreased $A5^-$ apoptotic events in CF AEC after 48 h, with significantly lower events in CF compared to non-CF AEC (D), significantly increased apoptotic bodies in non-CF AEC after 24 h (E), and significantly increased apoptotic bodies in non-CF and CF AEC following 48 h of RV1b infection (F). *$P < 0.05$.

Table 1. Expected staining of Annexin V and TO-PRO-3.

Populations	Annexin V	TO-PRO-3	FSC/SSC
Viable	Low	Low	Intermediate/high
Necrotic	High	High	Intermediate/high
$A5^+$ apoptotic	High	Intermediate	Intermediate/high
$A5^-$ apoptotic	Low	Intermediate	Intermediate/high
Apoptotic bodies	Intermediate	Low/intermediate	Low/low
Debris	Low	Low	Low

DISCUSSION

This study investigated the effectiveness of the gold standard A5/PI staining to assess viability, apoptotic, and necrotic cell death and compared the results to a novel flow cytometry analysis pipeline adapted to AEC, utilizing A5/TP3 staining combined with a seven-step gating strategy. While staining with A5/PI was able to differentiate apoptotic and necrotic cells within a sample, the lack of clarity about the double-positive population represents was of concern. There is no consensus whether the double-positive population represents apoptotic cells with permeabilized membranes or necrotic samples with exposed phosphatidylserine which then bind A5 [9]. Furthermore, recent data suggests that necrotic cells stain $A5^+/PI^-$ initially before becoming $A5^-/PI^+$ [13]. As a result, a novel flow cytometry method was adapted to AEC and assessed for its ability to differentiate viable, apoptotic, and necrotic events with more certainty [14]. The study by Jiang *et al*. (2016) utilized T cells, monocytes, squamous cells, endothelial cells, and fibroblasts but was successfully adapted to AEC in this manuscript. Furthermore, although A5 with PI or other membrane-exclusion dyes could detect primary necrosis, debris and apoptotic bodies were unable to be detected using the outlined method [14].

A large amount of apoptotic bodies were detectable after chemical induction of necrosis in a number of cell types [14]. The generation of apoptotic bodies was also observed in this study when using primary AEC following RV infection, with phenotypical differences observed between non-CF and CF AEC. As part of the homeostatic process in the airway, effective phagocytosis and removal of apoptotic cells termed efferocytosis [22] is vital to maintain the "immunologically silent" status commonly prescribed to apoptotic cells [23]. In the airway, this is performed by professional phagocytes such as macrophages and neutrophils [24], or *via* engulfment by non-professional phagocytes including AEC [25]. Since defective apoptotic responses have been observed in AEC and neutrophils in CF [5,26], reported accumulation of apoptotic cells in the CF airway may be suggestive evidence of defective efferocytosis [27]. Impaired phagocytic capacity in a number of cell types has been reported in CF [22,28]. Failure to successfully clear apoptotic cells can result in an immune response since apoptotic cells undergo secondary necrosis [29] and apoptotic cell disassembly. Interleukin-1 released by non-CF AEC during RV1b infection is associated with apoptosis [30], suggesting signaling may result from the immunological response to secondary necrosis and apoptotic breakdown of AEC. As apoptotic bodies can stimulate neutrophilic inflammation *via* IL-1α [17], it is important to elucidate the contribution of early apoptotic events during cell disassembly.

We were able to adapt the novel flow cytometry methodology utilizing A5/TP3 staining in conjunction with a seven-step gating analysis to differentiate viable, necrotic, and apoptotic events to an airway epithelial cell population after stimulation. Using this adapted flow and gating methodology, which can capture particles resulting from cells breaking down due to secondary apoptosis in a sample, we can have greater confidence in data generated when differentiating between viable, necrotic, and apoptotic cells. Utilizing AEC lines, comparable staining to the study by Jiang *et al*., (2016) was detected *via* flow cytometry [14]. After infection of AEC with RV confirmed *via* PCR, we were also able to observe decreased viable events, increased necrotic events, and increased apoptotic events in primary AEC. From the experiments conducted in this study, future work investigating cell death should be conducted utilizing A5/TP3 staining for differentiation between viable, necrotic, and apoptotic events *via* flow cytometry rather than the traditional A5/PI staining. After successfully adapting this methodology to primary AEC, there is now a robust approach to test whether there are phenotypic differences between the response of non-CF and CF AEC following RV infection and if the resultant inflammation is IL-1R driven. In the future, this methodology can be used successfully and with ease to investigate whether RV infection drives necrosis in the CF airway, and how it is linked to early life inflammation driven by IL-1R signaling observed *in vivo*. More broadly, this method can easily be adapted to other chronic airway diseases where mucus obstruction and cell death of airway epithelial cells is a typical observation including diseases such as asthma, chronic obstructive pulmonary disease, and idiopathic pulmonary fibrosis.

Acknowledgments

This study was performed on behalf of the Australian Respiratory Early Surveillance Team for Cystic Fibrosis (AREST CF) and the Western Australian Epithelial Research Program (WAERP). The full membership of AREST CF can be found at www.arestcf.org. The authors would like to thank the patients and their families in both the AREST CF and WAERP studies for their participation in this research. STM is funded by Cystic Fibrosis Australia and Cystic Fibrosis Western Australia. SMS is a NHMRC Practitioner Fellow. AK is a Rothwell Family Fellow.

References

1. Stick SM, Brennan S, Murray C, Douglas T, von Ungern-Sternberg BS, et al. (2009) Bronchiectasis in infants and preschool children diagnosed with cystic fibrosis after newborn screening. J Pediatr 155: 623-628. doi: 10.1016/j.

jpeds.2009.05.005. PMID: 19616787
2. Deschamp AR, Hatch JE, Slaven JE, Gebregziabher N, Storch G, et al. (2019) Early respiratory viral infections in infants with cystic fibrosis. J Cyst Fibros 18: 844-850. doi: 10.1016/j.jcf.2019.02.004. PMID: 30826285
3. van Ewijk BE, van der Zalm, M. (Marieke) , Wolfs TFW, Fleer A, Kimpen JLL, et al. (2008) Prevalence and impact of respiratory viral infections in young children with cystic fibrosis: prospective cohort study. Pediatrics 122: 1171-1176. doi: 10.1542/peds.2007-3139. PMID: 19047230
4. Gern JE, Dick EC, Lee WM, Murray S, Meyer K, et al. (1996) Rhinovirus enters but does not replicate inside monocytes and airway macrophages. J Immunol 156: 621-627. PMID: 8543813
5. Sutanto EN, Kicic A, Foo CJ, Stevens PT, Mullane D, et al. (2011) Innate inflammatory responses of pediatric cystic fibrosis airway epithelial cells: effects of nonviral and viral stimulation. Am J Respir Cell Mol Biol 44: 761-767. doi: 10.1165/rcmb.2010-0368OC. PMID: 21317379
6. Lötzerich M, Roulin PS, Boucke K, Witte R, Georgiev O, et al. (2018) Rhinovirus 3C protease suppresses apoptosis and triggers caspase-independent cell death. Cell Death Dis 9: 272-850. doi: 10.1038/s41419-018-0306-6. PMID: 29449668
7. Fritzsching B, Zhou-Suckow Z, Trojanek JB, Schubert SC, Schatterny J, et al. (2015) Hypoxic epithelial necrosis triggers neutrophilic inflammation via IL-1 receptor signaling in cystic fibrosis lung disease. Am J Respir Crit Care Med 191: 902-913. doi: 10.1164/rccm.201409-1610OC. PMID: 25607238
8. Montgomery ST, Dittrich AS, Garratt LW, Turkovic L, Frey DL, et al. (2018) Interleukin-1 is associated with inflammation and structural lung disease in young children with cystic fibrosis. J Cyst Fibros 17: 715-722. doi: 10.1016/j.jcf.2018.05.006. PMID: 29884450
9. Vermes I, Haanen C, Steffens-Nakken H, Reutelingsperger C (1995) A novel assay for apoptosis. Flow cytometric detection of phosphatidylserine expression on early apoptotic cells using fluorescein labelled Annexin V. J Immunol Methods 184: 39-51. doi: 10.1016/0022-1759(95)00072-i. PMID: 7622868
10. Faleiro L, Lazebnik Y (2000) Caspases disrupt the nuclear-cytoplasmic barrier. J Cell Biol 151: 951-959. doi: 10.1083/jcb.151.5.951. PMID: 11085998
11. Vanden Berghe, T. , Vanlangenakker N, Parthoens E, Deckers W, Devos M, et al. (2009) Necroptosis, necrosis and secondary necrosis converge on similar cellular disintegration features. Cell Death Differ 17: 922-930. doi: 10.1038/cdd.2009.184. PMID: 20010783
12. Rieger AM, Hall BE, Luong LT, Schang LM, Barreda DR (2010) Conventional apoptosis assays using propidium iodide generate a significant number of false positives that prevent accurate assessment of cell death. J Immunol Methods 358: 81-92. doi: 10.1016/j.jim.2010.03.019.
13. Sawai H, Domae N (2011) Discrimination between primary necrosis and apoptosis by necrostatin-1 in Annexin V-positive/propidium iodide-negative cells. Biochem Biophys Res Commun 411: 569-573. doi: 10.1016/j.bbrc.2011.06.186.
14. Jiang L, Tixeira R, Caruso S, Atkin-Smith GK, Baxter AA, et al. (2016) Monitoring the progression of cell death and the disassembly of dying cells by flow cytometry. Nat Protoc 11: 655-663. doi: 10.1038/nprot.2016.028. PMID: 26938116
15. Poon IKH, Chiu Y, Armstrong AJ, Kinchen JM, Juncadella IJ, et al. (2014) Unexpected link between an antibiotic, pannexin channels and apoptosis. Nature 507: 329-334. doi: 10.1038/nature13147. PMID: 24646995
16. Orlando KA, Stone NL, Pittman RN (2005) Rho kinase regulates fragmentation and phagocytosis of apoptotic cells. Exp Cell Res 312: 5-15. doi: 10.1016/j.yexcr.2005.09.012. PMID: 16259978
17. Berda-Haddad Y, Robert S, Salers P, Zekraoui L, Farnarier C, et al. (2011) Sterile inflammation of endothelial cell-derived apoptotic bodies is mediated by interleukin-1α. Proc Natl Acad Sci U S A 108: 20684-20689. doi: 10.1073/pnas.1116848108. PMID: 22143786
18. Zernecke A, Bidzhekov K, Noels H, Shagdarsuren E, Gan L, et al. (2009) Delivery of microRNA-126 by apoptotic bodies induces CXCL12-dependent vascular protection. Sci Signal 2: doi: 10.1126/scisignal.2000610. PMID: 19996457
19. Martinovich KM, Iosifidis T, Buckley AG, Looi K, Ling K, et al. (2017) Conditionally reprogrammed primary airway epithelial cells maintain morphology, lineage and disease specific functional characteristics. Sci Rep 7: 17971. doi: 10.1038/s41598-017-17952-4. PMID: 29269735
20. Lee W, Chen Y, Wang W, Mosser A (2015) Growth of human rhinovirus in H1-HeLa cell suspension culture and purification of virions. Methods Mol Biol 1221: 49-61. doi: 10.1007/978-1-4939-1571-2_5. PMID: 25261306
21. Bochkov YA, Palmenberg AC, Lee W, Rathe JA, Amineva SP, et al. (2011) Molecular modeling, organ culture and reverse genetics for a newly identified human rhinovirus C. Nat Med 17: 627-632. doi: 10.1038/nm.2358. PMID: 21483405
22. Vandivier RW, Henson PM, Douglas IS (2006) Burying the dead: the impact of failed apoptotic cell removal (efferocytosis) on chronic inflammatory lung disease. Chest 129: 1673-1682. doi: 10.1378/chest.129.6.1673. PMID: 16778289
23. Szondy Z, Sarang Z, Kiss B, Garabuczi , Köröskényi K (2017) Anti-inflammatory Mechanisms Triggered by Apoptotic Cells during Their Clearance. Front Immunol 8: 909. doi: 10.3389/fimmu.2017.00909. PMID: 28824635
24. Silva MT, Correia-Neves M (2012) Neutrophils and macrophages: the main partners of phagocyte cell systems. Front Immunol 3: 174. doi: 10.3389/fimmu.2012.00174. PMID: 22783254
25. Juncadella IJ, Kadl A, Sharma AK, Shim YM, Hochreiter-Hufford A, et al. (2012) Apoptotic cell clearance by bronchial epithelial cells critically influences airway inflammation. Nature 493: 547-551. doi: 10.1038/nature11714. PMID: 23235830
26. Gray RD, Hardisty G, Regan KH, Smith M, Robb CT, et al. (2017) Delayed neutrophil apoptosis enhances NET formation in cystic fibrosis. Thorax 73: 134-144. doi: 10.1136/thoraxjnl-2017-210134. PMID: 28916704
27. Vandivier RW, Fadok VA, Hoffmann PR, Bratton DL, Penvari C, et al. (2002) Elastase-mediated phosphatidylserine receptor cleavage impairs apoptotic cell clearance in cystic fibrosis and bronchiectasis. J Clin Invest 109: 661-670. doi: 10.1172/JCI13572. PMID: 11877474
28. Forrest OA, Ingersoll SA, Preininger MK, Laval J, Limoli DH, et al. (2018) Frontline Science: Pathological conditioning of human neutrophils recruited to the airway milieu in cystic fibrosis. J Leukoc Biol 104: 665-675. doi: 10.1002/JLB.5HI1117-454RR. PMID: 29741792
29. Sachet M, Liang YY, Oehler R (2017) The immune response to secondary necrotic cells. Apoptosis 22: 1189-1204. doi: 10.1007/s10495-017-1413-z.
30. Montgomery ST, Frey DL, Mall MA, Stick SM, Kicic A (2020) Rhinovirus infection is associated with airway epithelial cell necrosis and inflammation via interleukin-1 in young children with cystic fibrosis. Front Immunol 11: 596. doi: 10.3389/fimmu.2020.00596. PMID: 32328066

Supplementary information

Table S1. Demographics of the study population.

Figure S1. Infection of primary AEC with RV1b results in increased viral titer after 24 h.

Supplementary information of this article can be found online at http://www.jbmethods.org/jbm/rt/suppFiles/336.